Binding between Ground-State Aluminum Ions and Small Molecules: $Al^+ \cdot (H_2/CH_4/C_2H_2/C_2H_4/C_2H_6)_n$. Can Al^+ Insert into H_2?

Paul R. Kemper, John Bushnell, and Michael T. Bowers*

Department of Chemistry, University of California at Santa Barbara, Santa Barbara, California 93106-9510

Gregory I. Gellene

Department of Chemistry and Biochemistry, Texas Tech University, Lubbock, Texas 79409-1061

Received: May 1, 1998

Binding energies and entropies have been measured for the attachment of up to four H_2 ligands and six small hydrocarbons to ground-state Al^+ ions (^1S, $3s^2$). Bond energies are typically very weak compared with analogous transition metal ion or the isovalent boron ion systems. Bond energies for the first ligand addition to Al^+ are 1.4 (H_2), 6.1 (CH_4), 9.3 (C_2H_6), 14.0 (C_2H_2), and 15.1 kcal/mol for C_2H_4. The origin of the weak bonding lies primarily in the large, repulsive 3s orbital, which prevents close approach by the ligands. In addition, the lack of low-energy acceptor orbitals on the Al^+ ion minimizes electron donation to the metal ion and also reduces the Al^+/ligand attraction. Finally, the lack of low lying, occupied π-type orbitals prevents donation from the Al^+ to the σ^* orbitals on the ligands. A very detailed theoretical examination of the $Al^+(H_2)_n$ cluster energetics was also made. The purpose was to investigate the possibility of insertion by the Al^+ into the H−H bond via σ bond activation, as is found with the isovalent B^+ ion. The calculations showed that the inserted $HAlH^+$ ion is stable but that its formation is endothermic by 10.9 kcal/mol with respect to the separated reactants. The inserted $HAlH^+(H_2)_2$ ion, however, appears to be almost isoenergetic with the uninserted $Al^+(H_2)_3$ isomeric cluster.

Introduction

The bonding of the aluminum ion (Al^+, ^1S, $3s^2$) with inorganic and organic ligands has received limited attention in the literature. The very few thermochemical bond energy measurements include those of Dalleska et al.[1] of the $Al^+(H_2O)_{1-4}$ bond energies and theoretical and low-pressure equilibrium studies of the $Al^+ + C_6(H/D)_6$ and HCN systems by Stöckigt et al.[2,3] Uppal and Staley[4] have examined the equilibrium exchange of ligands between $Al^+X + Y \leftrightarrow Al^+Y + X$ and obtained relative bond energies, but no absolute values. Hodges et al.[5] observed association between Al^+ and various alkyl halides, ethers, ketones, and alcohols, but again, no thermochemical results were reported. Jarrold and Bower[6] have investigated the chemisorbtion of D_2 molecules on Al_n^+ clusters. No D_2 addition was observed for $n < 8$, however, probably due to the 0.2−0.3 eV minimum energy of their ion beam. Theoretical investigations of Al^+ ligation have been far more numerous. Bauschlicher and co-workers have calculated energies for Al^+ bonding with CO, H_2O, NH_3, and CN,[7] as well as a number of different aldehydes, ketones, and alcohols.[8] Stöckigt and Hrušák have examined the $Al^+-C_6H_6$ system[2] as well as $Al^+-\pi$ interactions[9] and the different possible isomers of the $AlC_2H_2^+$ ion.[10] More recently, Stöckigt et al.[11] published high-level theoretical calculations of the bond dissociation energies of the Al^+-$(C_2H_{2,4,6})$ ions together with limited energy bracketing and equilibrium experiments on the same ions. In all these investigations, no discussion of the $Al^+(H_2)_n$ ions has been presented.

The reaction of Al^+ with H_2 has assumed greater interest due to recent experiments involving B^+ and H_2. Both dePuy's[12] and our experiments[13] have shown that while the B^+ atomic ion forms only weakly bound, electrostatic clusters with H_2, the inserted HBH^+ ion forms strong, largely covalent bonds with up to two additional H_2 ligands. Further, both our experiments[13] and the extensive theoretical calculations of Sharp and Gellene[14] show that the barrier for conversion of the uninserted, electrostatic $B^+(H_2)_n$ clusters to the inserted, covalent $HBH^+(H_2)_{n-1}$ clusters decreases sharply as the number of H_2 ligands increases. This effect is dramatic, with the activation energy for $B^+H_2 \rightarrow HBH^+$ equal to ∼56 kcal/mol, while that for $B^+(H_2)_3 \rightarrow HBH^+(H_2)_2$ is equal to ∼3 kcal/mol. This reduction is due to an optimal positioning of the molecular orbital nodal planes in the $B^+(H_2)_3$ ion, allowing a very facile insertion. Since both B^+ (^1S, $2s^2$) and Al^+ (^1S, $3s^2$) are isovalent, the $Al^+(H_2)_n$ clusters might be expected to behave similarly and possibly undergo insertion to form the $HAlH^+(H_2)_{n-1}$ covalent clusters. The present experiments with H_2 were performed largely to explore this possibility. Bond dissociation energies for the corresponding Al^+/methane/ethane/ethylene/acetylene complexes were also measured to provide a check on the theoretical results of Stöckigt et al.,[11] which disagreed slightly with their FTICR equilibrium results.

Experimental Techniques

The Instrument. The equilibrium experiments were performed on an ion source/quadrupole/high-pressure reaction cell/quadrupole/detector type instrument, which has been described previously.[15] The aluminum ions were formed by either glow discharge sputtering of an aluminum rod in an argon atmosphere or by surface ionization of $Al(CH_3)_3$ on a hot rhenium ribbon

10.1021/jp982090o CCC: $15.00
Published on Web 07/15/1998

filament. The differences observed are discussed below. The quadrupole mass-selected Al^+ ions were injected through a 0.5 mm orifice into the gas cell, which contained 3−10 Torr of the pure ligating gas (H_2, CH_4, etc.). Injection energies were typically 20−30 eV; changing this energy from 20−100 eV had no effect on the experimental results. Once in the cell, the Al^+ ions quickly thermalize and form an equilibrium distribution of the $Al^+{\cdot}L_n$ clusters. The ions were moved through the cell with a small electric field, and a small fraction exited through a second 0.5 mm orifice. Sampling through this orifice has been shown to be nonselective. The resulting $Al^+{\cdot}L_n$ intensities are mass analyzed in a second quadrupole and detected. The ratios of the different clusters, together with the ligating gas pressure and temperature, are used to calculate K_p° and ΔG_T° according to eqs 1 and 2.

$$K_p^\circ = \frac{Al^+(L)_n \times 760}{Al^+(L)_{n-1} \times p_L} \quad (1)$$

$$\Delta G_T^\circ = -RT \ln K_p^\circ \quad (2)$$

$$\Delta G_T^\circ = \Delta H_T^\circ - T\Delta S_T^\circ \quad (3)$$

These equilibrium measurements are repeated at different temperatures (from 77 to 700 K in this series of experiments). The resulting ΔG_T° vs T plots are linear over the experimental temperature range for all experiments reported here. Extrapolation to 0 K yields an intercept equal to ΔH_T° and a slope equal to ΔS_T°. The experimental ΔH_T° values are converted to ΔH_0° (≡−bond dissociation energy, or BDE) using theoretical geometries and harmonic vibrational frequencies. Specifically, these theoretical parameters are used to calculate a theoretical ΔG_T° vs T curve, which is then matched to the experimental curve by varying the lower vibrational frequencies and ΔH_0° value. The theoretical geometries are not varied since they are sufficiently well-known that no reasonable variation will affect the theoretical ΔG_T°. The frequencies, together with an experimental mass discrimination factor, are varied over a wide range to determine the range of possible bond energies. The uncertainty in ΔH_0° is about 10% of the weak bond energies obtained here. A detailed discussion of this proceedure and possible errors is given elsewhere.[16] According to the manufacturer, the C_2H_2, C_2H_4, and C_2H_6 gas purities were 99.9%, while those of H_2 and CH_4 were 99.999%. The lower purities caused some problems, especially in measuring the second ligand addition, and resulted in a greater uncertainty. The ΔS_T° numbers are typically accurate to ±2 cal/(mol·K). These association entropies are often neglected, but are important indicators of new solvation shells,[17] spin changes,[18] and other changes in bonding.

Al^+ Excited Electronic States. The Al^+ ion has a single metastable state (the ^3P, 3s3p) with an excitation energy of 107 kcal/mol. Since this state has the potential to promote endothermic reactions, it is important to determine if it is present. As noted, two methods were used to form the Al^+ ions: glow discharge and surface ionization (SI). Electronic-state chromatography (ESC)[19] of the Al^+ ions formed by glow discharge did show the presence of two electronic states. When SI was used, however, only the state with the larger mobility was detectable. Since SI forms a Boltzmann distribution of ion energies at the temperature of the ionization filament (∼2500 K), we do not expect any measurable ^3P population. This indicates that the excited ^3P is the state with the lower mobility. This is perhaps counterintuitive, but removing a paired electron from the 3s orbital reduces the size of the 3s orbital by reducing electron−electron repulsion. This in turn allows a closer Al^+−He approach, increasing the Al^+−He attraction and giving rise to the lower mobility. These same effects are found in ESC studies of the transition metals.[19] The Al^+−He interaction is controlled by the 3s orbital, and the electron in the smaller 3p orbital has little influence.

The important result for the present experiments is that no difference in reactivity was found between the Al^+ ions formed by glow discharge and those formed by SI. This indicates that, although no measurable deactivation was seen in the He buffer gas, the highly excited Al^+ ions are efficiently deactivated by all the neutrals investigated here.

Computational Methods. The structure and binding energies of the electrostatic complexes, $Al^+(H_2)_n$ (n = 1−4), and the corresponding cluster ions built on the inserted $HAlH^+$ core, $HAlH^+(H_2)_{n-1}$ (n = 1−3), have been determined by ab initio calculations at the MP2 (frozen core electrons) level using the aug-cc-pVZT basis set.[20] This basis set is of triple-ζ quality augmented by diffuse functions. For aluminum, the basis set consists of a (15s9p2d1f) set of primitive Gaussian functions contracted to [5s4p2d1f] and augmented by an uncontracted (1s1p1d1f) set of diffuse functions. For hydrogen, the basis set consists of a (7s2p1d) primitive set contracted to [3s2p1d] and augmented by a (1s1p1d) set of uncontracted diffuse functions. Pure spherical harmonic functions were used with this basis set. In these calculations, analytical first derivatives were used to optimize geometric structures to a residual rms force of less than 10^{-6} hartree/bohr. The structures were identified as local minima by the presence of all real harmonic frequencies, as determined from analytical second derivatives.

Additionally, the $Al^+(H_2)_n$ and $Al^+(CH_4)_n$ (n = 1−2) ions were examined with density functional theory using the B3LYP functional and the D95++(d,p) basis set. This set is of double-ζ quality augmented by diffuse functions on both the heavy atoms and hydrogen. For aluminum, the basis set consisted of a (12s8p1d) set of primitive Gaussian functions contracted to [6s4p1d] and augmented by an uncontracted (1s1p) set of diffuse functions. For hydrogen, the basis set consisted of a (4s1p) primitive set contracted to [2s1p] and augmented with a (1s) uncontracted diffuse function. A (9s5p1d) primitive basis set augmented with (1s1p) diffuse functions was used for carbon. The Al−H_2 bond lengths from the DFT calculations agreed well with the MP2 results; however the calculated BDE (0.64 kcal/mol) was far smaller than both experiment (1.35 kcal/mol) and the MP2 calculation (1.06 kcal/mol). In addition, the geometry of the $Al^+(H_2)_2$ ion determined by DFT had an H_2−Al^+−H_2 bond angle of 163° (i.e., nearly linear), while the MP2 calculation found a 65° angle. The reasons for the differences are not clear, but the MP2 results were deemed more reliable. Both the MP2 and the DFT calculations were performed using the GAUSSIAN 94 suite of programs.[21]

Results and Discussion

$Al^+(H_2)_n$. The ΔG_T° vs T data for the first four H_2 additions to the Al^+ core ion are shown in Figure 1. The third and fourth additions could only be observed at the coldest temperatures available (77 K) and no ΔS_T° data are available. The resulting ΔH_T° and ΔS_T° values are listed in Table 1 along with the ΔH_0° (−bond dissociation energy) values from our statistical mechanical fit to the data. The bond energies from the present MP2/aug-cc-pVTZ calculations are listed in Table 1. The calculated structures are shown in Figure 2. The coordinates R, r_{H_2}, and θ_{R,H_2} are used to denote the distance between Al^+ and the midpoint of an H_2 bond (BMP), the H−H bond length, and the angle between R and r_{H_2}, respectively.

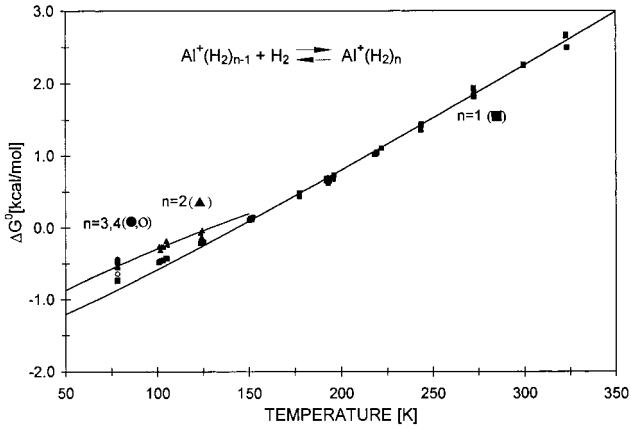

Figure 1. Plot of free energy vs temperature data for the $Al^+(H_2)_{n-1} + H_2 \rightarrow Al^+(H_2)_n$ association reactions.

It is clear from both theory and experiment that these $Al^+(H_2)_n$ clusters are weakly bound, electrostatic clusters. The very small bond energies (≤1.5 kcal/mol, Table 1), together with the long Al^+-H_2 bond length (~3.0 Å) illustrate the weak, electrostatic nature of the interaction. The almost unperturbed H−H bond length and vibrational frequency show that the H_2 ligands are essentially intact H_2 molecules. The majority of the Al^+-H_2 attraction is due to the charge-induced dipole (CID) and the charge quadrupole (CQ) potentials. The charge quadrupole attraction is the origin of the "T" structure ($\theta_{R,H_2} = 90 \pm 1°$; C_{2v} symmetry) present in Al^+H_2 (Figure 2). As shown in Table 1, agreement between theory and experimental bond energies is good, with the MP2 calculation generally describing about 75% of the bonding.

As a first approximation, bonding in these ions can be viewed as a balance between the CID and CQ attractions and the Pauli (electron−electron) repulsion between the filled Al^+ 3s and the H_2 σ orbitals. The origin of the weak bonding lies primarily in the large amount of repulsion present. Because the 3s is a large, filled orbital, repulsion is greater than that present in the corresponding complexes formed with transition metal ions. Further, the lack of low lying p or d orbitals impedes polarization of the 3s orbital away from the ligands. Finally, the lack of low-energy acceptor orbitals, together with the filled 3s orbital, prevents significant electron donation from the H_2 ligands to stabilize the Al^+ ion. Together these factors give rise to the very small bond dissociation energies that we observe.

This simple view of the $Al^+(H_2)_n$ interaction is largely, but not entirely, complete. The Al^+ ion does not behave as a simple point charge. Because the repulsion due to the large filled 3s orbital does largely control the bonding in these systems, theory indicates that some polarization of the 3s by the $3p_z$ orbital does occur to reduce this repulsion. By mixing the 3s and $3p_z$, some 3s electron density is moved to the side of the ion opposite the H_2 ligand. This effect is minimal compared to the 3d/4s hybridization which occurs in the corresponding transition metal−H_2 complexes[22] (where the 4s and 3d orbital energies are similar) but is sufficient to control the geometries of the $Al^+(H_2)_n$ ions. This is shown in the geometries of the larger $Al^+(H_2)_n$ clusters, where the second and third H_2 ligands add at approximately 65° to the existing ligands (Figure 2). This geometry preserves the benefits of the existing 3s/3p polarization present in the reactant clusters by adding additional ligands away from the polarized electron clouds. The quadrupole−quadrupole attraction between the H_2 ligands may also play a role, especially in the near perpendicular relative orientation of the H_2 ligands. The theoretical structures of analogous $Mn^+(H_2)_n$ and $Zn^+(H_2)_n$ systems (which contain a 4s electron) show a 90° orientation of the H_2 ligands.[23] This, and the greater BDEs found in these ions, may be due to the lower energy of the 4p orbitals, which allows greater polarization of the s electron.

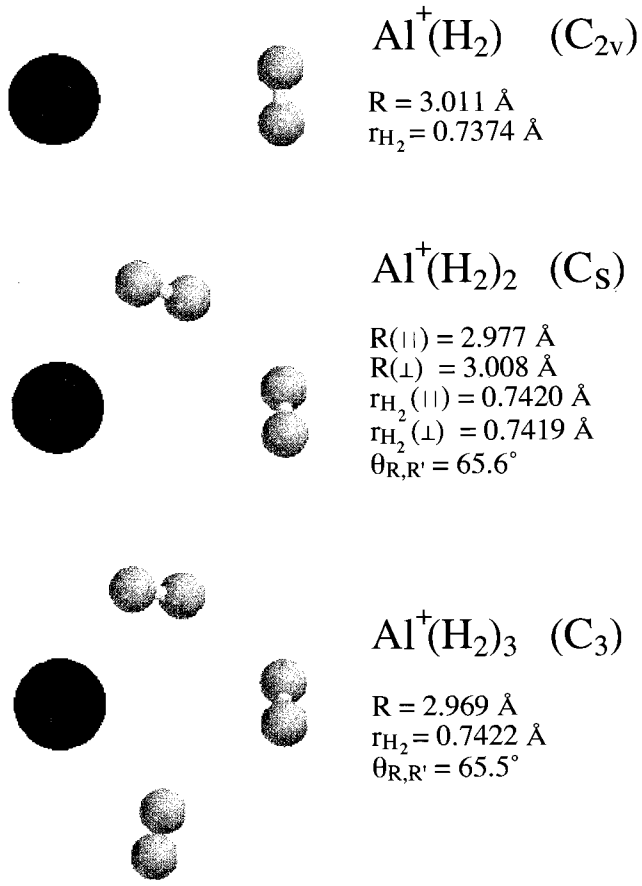

Figure 2. Geometries of the electrostatically bound $Al^+(H_2)_n$ cluster ions calculated at the MP2 aug-cc-pVZT level. Bond lengths are in angstroms.

The Mg^+H_2 ion (Mg^+: ^2S, $3s^1$) has been studied extensively by Bauschlicher and co-workers.[24−26] They find the bonding to be almost entirely electrostatic (as in Al^+H_2) with a BDE of 1.5 kcal/mol. This Al^+/Mg^+ BDE ratio of ~0.7 is largely independent of ligand (see below). The $Mg^+(H_2)_2$ cluster was

TABLE 1: Data Summary for $Al^+(H_2)_n$ Clusters[a]

product ion[a]	experiment				theory		
$Al^+(H_2)_n$	BDE[b,c]	$-\Delta H_T^{\circ b}$	$-\Delta S_T^{\circ d}$	T^e	symmetry	D_e[b]	D_0[b]
$Al^+(H_2)$	1.35 ± 0.15[f]	2.1 ± 0.1	14.5 ± 1.5	240 ± 100	C_{2v}	1.2,[g] 1.75[h]	0.64,[g] 1.06[h]
$Al^+(H_2)_2$	1.10 ± 0.15[f]	1.24 ± 0.1	9.2 ± 1.5	100 ± 25	C_{2v},[g] C_s[h]	1.06,[g] 1.86[h]	0.45,[g] 0.81[h]
$Al^+(H_2)_3$		~1.2[i]		77		2.00[h]	0.68[h]
$Al^+(H_2)_4$		~1.2[i]		77		1.81[h]	0.66[h]

[a] For the association process $Al^+(H_2)_{n-1} + H_2 \rightarrow Al^+(H_2)_n$. [b] In kcal/mol. [c] Bond dissociation energy (BDE) = $-\Delta H_0^\circ$. [d] In cal/(mol K). [e] In Kelvin, ± refers to temperature range, not uncertainty. [f] Fitting with theoretical frequencies and geometries. [g] DFT geometries. [h] MP2/aug-cc-pVZT geometries. [i] Fit by correspondence with second cluster; not enough data for ΔS and ΔH measurement.

also studied, and a bent geometry, strikingly similar to $Al^+(H_2)_2$ (Figure 2) was also found for the ground state.[25] The H−H bonds are again oriented 90° with respect to each other; the $H_2-Al^+-H_2$ angle is slightly greater (72.5° vs 65° in Al^+).

As noted above, one motivation in studying the $Al^+(H_2)_n$ clusters was comparison with the $B^+(H_2)_n$ systems reported earlier.[12−14] Because the ions are isovalent (B^+: [He]$2s^2$; Al^+: [Ne]$3s^2$), they are expected to show similar structures and trends in bond energy. This is in fact the case; both the $B^+(H_2)_n$ and $Al^+(H_2)_n$ ions are weakly bound electrostatic clusters with bent geometries. The H_2 ligands bind more strongly to $B^+(H_2)_{n-1}$ however, because the smaller 2s orbital allows a closer approach ($R \sim 2.3$ Å vs ∼3.0 Å in Al^+). This in turn increases the CID and CQ attractions, and bond energies of 3−4 kcal/mol are found in contrast to the very weak 1−1.4 kcal/mol values in $Al^+(H_2)_{n-1}$ (Table 1). Because the $^1S-{}^1P$ promotion energy is actually higher in the B^+ case (209.9 vs 171.1 kcal/mol[27]) and because this energy controls the cost of polarizing the s orbital, it seems that the decrease in bond energies in the $Al^+(H_2)_n$ ions is due purely to the increased size of the 3s orbital.

Probably the most interesting comparison between aluminum and boron concerns the possibility of insertion into the H−H bond to form $HAlH^+$ ions. For this reason we focused much of our theoretical efforts here. The inserted HBH^+ ion is a strongly bound 2s2p hybrid which can add two additional, relatively strongly bound H_2 ligands to form an $HBH^+(H_2)_2$ terminal ion with a quasi sp^3 hybridization.[12−14] Although formation of the HBH^+ ion is 55.9 kcal/mol exothermic with respect to the separated reactants, there is a barrier of 56 kcal/mol to the simple bimolecular insertion.[14] This insertion reaction is unusual, however, and experiments and theory have shown that the size of the insertion barrier as well as the nature of the transition state are both very strong functions of the number of H_2 ligands.[13,14] In fact, when three H_2 ligands are added to B^+, the insertion barrier height shrinks to ∼3 kcal/mol due to a proper alignment of the nodal planes between the filled molecular orbitals.[14] Because in our relatively high-pressure, thermal energy experiments insertion proceeds from the $B^+(H_2)_3$ ion, increasing its population among the $B^+(H_2)_n$ clusters increases the rate of insertion. In addition, because the uninserted H_2 ligands are weakly bound to B^+, the $B^+(H_2)_3$ population and the rate of insertion both increase as the temperature is lowered. Thus in the B^+-H_2 system, insertion could be detected by the nonequilibrium conversion of the $B^+(H_2)_n$ clusters to the $HBH^+(H_2)_2$ terminal ion at low temperatures. (Remember that the inserted HBH^+ ion strongly binds to two additional H_2 ligands.) Formation of the corresponding $HAlH^+(H_2)_n$ ions would be extremely interesting, and significant experimental and theoretical efforts were made to observe insertion in the Al^+-H_2 system. It was not observed experimentally, however, for reasons that are now clear from our calculations. The root cause of the difference between B^+ and Al^+ is the weaker bonds formed by the Al^+ ion. First, the Al^+-H bond strength is only ∼45 kcal/mol (vs ∼56 kcal/mol for B^+-H). (Bond strength data for the inserted $HAlH^+(H_2)_n$ ions are summarized in Table 2; geometries and bond lengths are shown in Figure 3.) This lower bond strength has several consequences. First, formation of the bare $HAlH^+$ ion is actually endothermic (by 10.9 kcal/mol, with respect to the separated reactants), unlike the boron case, where formation is 55.9 kcal/mol exothermic.[14] This difference is reflected in the Al^+-H bond length (1.55 Å vs 1.17 Å in B^+-H). Our calculations do indicate that the $HAlH^+$ ion occupies a local minimum, however, and its isolation is at least theoretically possible. Second, although $HAlH^+$ does add two additional H_2 ligands with bond strengths greater than the electrostatic Al^+-H_2, the bonds are only 5.4 and 5.1 kcal/mol (Table 2), far less than the 14.7 and 18.1 kcal/mol values found with HBH^+. (Again this is seen in the bond lengths with $R_{Al} \sim 2.08$ Å and $R_B \sim 1.33$ Å.) The net result is that the inserted $HAlH^+(H_2)_2$ and the uninserted $Al^+(H_2)_3$ ions are very similar in energy. Our best calculation, including zero point energies, shows the electrostatic cluster to be approximately 3 kcal/mol lower in energy than the inserted isomer (Table 2). Consequently, although some inserted $HAlH^+(H_2)_2$ *may* be formed in our experiment, it will not be the favored terminal ion due to unfavorable energetics and the small populations of the electrostatic $Al^+(H_2)_3$ reactant ion (due to the small $Al^+(H_2)_n$ binding energies). As in the B^+ case, the barrier to insertion decreases

TABLE 2: Summary of Theoretical Results for Inserted $HAlH^+(H_2)_n$ Clusters[a,b]

product ion[a]	symmetry	D_e[b,c]	D_0[b,c]	$E_{inserted} - E_{electrostatic}$[d] D_e	$E_{inserted} - E_{electrostatic}$[d] D_0
$HAlH^+$	$D_{\infty h}$	−9.6	−10.9	11.4	12.0
$HAlH^+(H_2)$	C_{2v}[e]	8.4	5.4	4.8	7.4
$HAlH^+(H_2)_2$	C_{2v}[f]	8.4	5.1	−1.6	3.0

[a] For the association process $HAlH^+(H_2)_{n-1} + H_2 \rightarrow HAlH^+(H_2)_n$. Negative energies correspond to an endothermic process. [b] Calculated at the MP2/aug-cc-pVZT level. [c] In kcal/mol. [d] For the insertion process $Al^+(H_2)_n \rightarrow HAlH^+(H_2)_{n-1}$. Positive energies correspond to an endothermic process. [e] Planar structure, see text. [f] Quasi tetrahedral structure, see text.

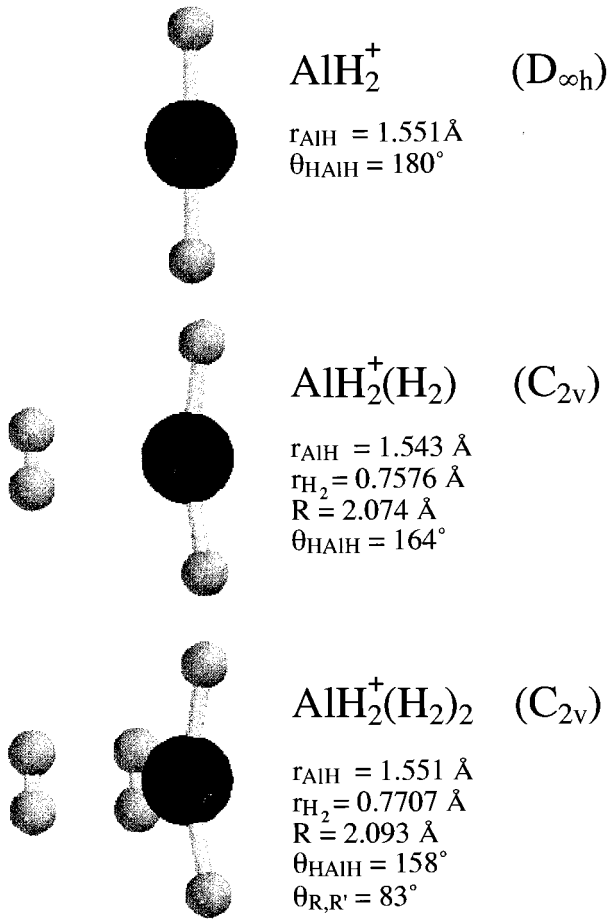

Figure 3. Geometries of the covalently bound $HAlH^+(H_2)_n$ ions calculated at the MP2 aug-cc-pVZT level. Bond lengths are in angstroms.

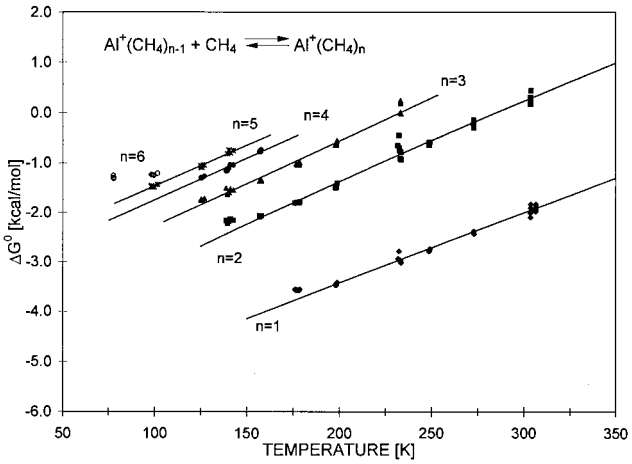

Figure 4. Plot of free energy vs temperature data for the $Al^+(CH_4)_{n-1} + CH_4 \rightarrow Al^+(CH_4)_n$ association reactions.

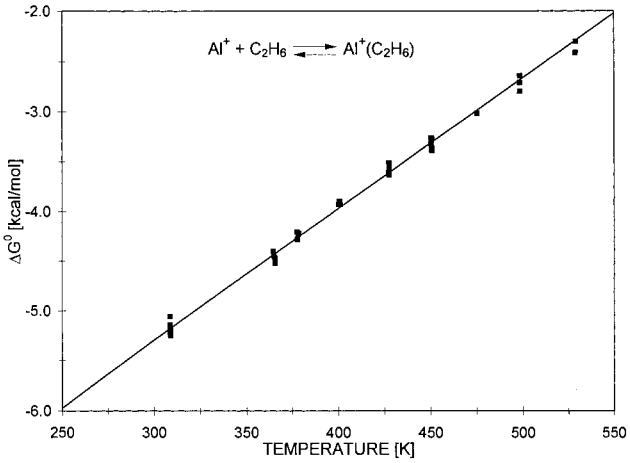

Figure 5. Plot of free energy vs temperature data for the $Al^+ + C_2H_6 \rightarrow Al^+C_2H_6$ association reaction.

sharply with H_2 ligation, and a detailed description of the insertion transition states in the different $Al^+(H_2)_n$ ions is in preparation.[28]

$Al^+(CH_4)_n$. The ΔG_T° vs T data for the addition of H_2 to $Al^+(CH_4)_{n-1}$ clusters are shown in Figure 4. The experimental results (ΔH_T°, ΔS_T°, and bond dissociation energy) are listed in Table 3 along with a summary of the theoretical results of Stöckigt et al.[11] and our DFT calculations. The statistical mechanical fit for the first cluster was done with the geometries and vibrational frequencies of Stöckigt et al.[11,29] The geometries for the larger clusters were estimated from these and from our calculations on the second cluster, which indicated a 90° ligand angle. Vibrational frequencies were estimated from those of the first cluster using a square-root scaling of the reduced mass and bond strength. These parameters were varied widely to determine the precision of the results. The resulting experimental bond dissociation energies range from 6.05 to 4.0 kcal/mol for the first three ligands and drop to about 3.0 kcal/mol for the last three. The first solvation shell thus appears to contain six CH_4 ligands. These Al^+-CH_4 dissociation energies are much larger than the H_2 values (~1.4−1 kcal/mol) but far weaker than the CH_4 interactions with the Co^+ and Fe^+ $3d^8$ and $3d^7$ valence configurations (respectively), which are greater than 20 kcal/mol,[30,31] or that with Ti^+ ($3d^3$), which is 19.3 kcal/mol.[32] This difference clearly illustrates the effect of the repulsive 3s orbital but also the importance of low lying, empty orbitals to reduce repulsive interactions and accept electron density. Interestingly the Mg^+-CH_4 interaction is calculated to be very similar to the Al^+-CH_4, with a bond energy of 6.3−7.6 kcal/mol.[33,34] It might seem that removing one of the repulsive 3s electrons (Mg^+: ^2S $3s^1$) would make a more substantial difference; however the change in 3s orbital size is minimal, and, as in the Al^+ ion, no low-energy d or p orbitals are available.

Stöckigt et al.[11] examined the Al^+-CH_4 interaction at the HF, MP2, and QCISD(T) levels and found a bond energy of 5.2 kcal/mol for the first CH_4 ligand binding to Al^+ (at the QCISD(T) level), in good agreement with our lower level DFT result of 4.8 and the experimental value of 6.05 kcal/mol. All calculations show the Al^+ ion to approach three H atoms on the CH_4 with an η^3 coordination (C_{3v} symmetry); the QCISD(T) Al−C bond length was 3.04 Å (there appears to be a misprint in the HF and MP2 bond lengths shown in Figure 1 of ref 11). The calculations also show the CH_4 ligand to be essentially unperturbed from the free reactant. Stöckigt et al. found also that ~95% of the binding between Al^+ and CH_4 was due to the charge-induced dipole (CID) attraction. The covalent component of the attraction was due primarily to donation from the 3s orbital on Al^+ to the σ^* orbital of the C−H bond in line with the C−Al^+ bond and from the σ orbital of that same C−H bond into the 3pσ orbital on Al^+ and, finally, donation from the three closest CH σ orbitals to the 3pπ orbitals. The very small size of the total covalent interaction is a direct consequence of the filled 3s orbital and the high energy required to access the empty 3p orbitals.

Very limited DFT calculations were done on the second cluster ($Al^+(CH_4)_2$) and are summarized in Table 3. They show a drop in D_e from 5.1 to 2.4 kcal/mol, somewhat greater than the experimental decrease from 6.05 to 4.8 kcal/mol. A bent geometry (C−Al−C angle ~90°) was lowest in energy. These results are similar to those found for the $Al^+(H_2)_n$ clusters and result from the same 3p/3s polarization effects. In general the $Al^+(CH_4)_n$ and $Al^+(H_2)_n$ ions exhibit very similar interactions.

TABLE 3: Data Summary for $Al^+(CH_4)_n$ Clusters[a]

product ion	experiment				theory		
	BDE[b]	$-\Delta H_T^{\circ b}$	$-\Delta S_T^{\circ c}$	T^d	symmetry	D_e[b]	D_0[b]
$Al^+(CH_4)$	6.05 ± 0.3[e]	6.2 ± 0.3	13.9 ± 1.5	240 ± 60	C_{3v}	5.1[f]	4.8,[f] 5.2[g]
$Al^+(CH_4)_2$	4.80 ± 0.3[e]	4.63 ± 0.2	16.2 ± 1.5	225 ± 75	C_s[h]	2.9[f]	
$Al^+(CH_4)_3$	4.04 ± 0.3[i]	4.05 ± 0.4	17.5 ± 1.5	180 ± 60			
$Al^+(CH_4)_4$	3.2 ± 0.6[i]	3.5 ± 0.5	17.0 ± 2	150 ± 25			
$Al^+(CH_4)_5$	3.0 ± 0.5[i]	3.1 ± 0.3	16.5 ± 2	120 ± 20			
$Al^+(CH_4)_6$	~2.8[j]	~2.9		77			

[a] For the association process $Al^+(CH_4)_{n-1} + CH_4 \rightarrow Al^+(CH_4)_n$. [b] In kcal/mol; the bond dissociation energy (BDE) = $-\Delta H_0^\circ$. [c] In cal/(mol K). [d] In Kelvin, ± refers to temperature range, not uncertainty. [e] Fitting with theoretical frequencies and geometries. [f] DFT geometries. [g] Single-point calculation at the QCISD(T)/6-311+G(3df,2p) level; D_0 calculated at 0 K; see ref 11. [h] CH_4−Al−CH_4 angle ~90°; see text. [i] Fitting with ΔC_p correction, error small at low temperature. [j] Fit by correspondence with fifth cluster; not enough data for ΔS and ΔH measurement.

TABLE 4: Data Summary for $Al^+(C_2H_{2,4,6})_n$ Clusters[a]

	experiment				theory	
ion	BDE[b]	$-\Delta H_T^{\circ b}$	$\Delta S_T^{\circ c}$	T^d	symmetry	$D_0{}^b$
$Al^+(C_2H_6)$	9.3 ± 0.5^e	9.2 ± 0.4	13.0 ± 1.5	425 ± 110	$C_s{}^f$	8.5^g
					$C_{3v}{}^h$	8.4^g
$Al^+(C_2H_4)$	14.9 ± 0.8^e	15.5 ± 0.8	18.5 ± 2	600 ± 125	C_{2v}	13.6^g
$Al^+(C_2H_4)_2$		~ 9		425		
$Al^+(C_2H_2)$	14.0 ± 1.0^e	14.9 ± 1.0	16.5 ± 2	625 ± 100	C_{2v}	13.2^g
$Al^+(C_2H_2)_2$	13.6 ± 1.5^e	14 ± 2.5	~ 16	575 ± 75		

[a] For the association process $Al^+(C_2H_x)_{n-1} + C_2H_x \rightarrow Al^+(C_2H_x)_n$. [b] In kcal/mol; the bond dissociation energy (BDE) $= -\Delta H_0^\circ$. [c] In cal/(mol K). [d] In Kelvin, $\pm$ refers to temperature range, not uncertainty. [e] Fitting with theoretical frequencies and geometries. [f] Side-on geometry. [g] Single-point calculation at the QCISD(T)/6-311+G(3df,2p) level; D_0 calculated at 0 K; see ref 11. [h] End-on geometry.

$Al^+C_2H_6$. Figure 5 shows the ΔG_T° vs T data for the addition of C_2H_6 to Al^+. The experimental results (ΔH_T°, ΔS_T°, and bond dissociation energy) are listed in Table 4. Theoretical results from Stöckigt et al.[11] are also shown, and the agreement between theoretical and experimental dissociation energies (8.5 and 9.4 kcal/mol, respectively) is very good. The geometries and vibrational frequencies used in our analysis were taken from Stöckigt et al.[11,29] Data could only be taken for one C_2H_6 ligand due to water contamination problems. Theory finds two very different structures with nearly identical bond dissociation energies for the ground state of the $Al^+C_2H_6$ ion: C_2H_6 side-on (C_s, η^3, BDE = 8.5 kcal/mol) and C_2H_6 end-on (C_{3v}, η^3, BDE = 8.4 kcal/mol). The $Al^+-C_2H_6$ interaction in both these structures is again largely electrostatic and the increased BDE of 9.4 kcal/mol (relative to 6.05 kcal/mol with CH_4) is due mainly to the increased polarizability of the ligand. Stöckigt et al.[11] estimate that greater than 90% of the attraction comes from the charge-induced dipole and charge quadrupole potentials and that the small covalent components are almost identical to those found with the CH_4 ligand (discussed above). Both the end-on and side-on structures have an η^3 coordination to Al^+ with an interaction nearly identical to that in Al^+-CH_4, although the Al−C bond distances are ∼7% shorter, reflecting the greater attraction.

The $Mg^+-C_2H_6$ interaction has been examined by Partridge et al.,[33] who found only an end-on structure. Comparing the Mg^+-CH_4 calculations in refs 33 and 34, it seems likely that the calculated $Mg^+-C_2H_6$ dissociation energy of 9.7 kcal/mol in ref 26 would increase ∼1.5 kcal/mol with a higher level of theory. If true, the $Mg^+-C_2H_6$ binding is similar to but slightly greater than that found in $Al^+-C_2H_6$. As noted above, the same correspondence is seen with the H_2 and CH_4 ligands.

$Al^+(C_2H_4)_n$. The experimental free energy data for the first two additions of C_2H_4 to Al^+ are shown in Figure 6. Water contamination again reduced the temperature range over which data for the second cluster could be taken. The entropy associated with this limited data was deemed unreliable and the ΔH_T° was derived by comparison with the first cluster. The ΔH_T° and ΔS_T° values along with the bond dissociation energies from our statistical mechanical fit are listed in Table 4. Again, the geometries and vibrational frequencies used were taken from Stöckigt et al.[11,29] and their D_e and D_0 values also listed in Table 4. The theoretical D_0 of 12.9 kcal/mol represents ∼85% of the present experimental bond dissociation energy of 15.1 kcal/mol. The lowest energy structure has the C_2H_4 bonded side-on to the Al^+ with the C_2H_4 plane perpendicular to the C−Al−C plane (C_{2v} symmetry). The Al−C distances are 2.85 Å: slightly shorter than those in $Al^+C_2H_6$ (∼3.0 Å). Very little distortion of the C_2H_4 occurs in forming the complex.

A substantial increase in bond energy occurs when C_2H_4 is substituted for C_2H_6 (15.1 vs 9.3 kcal/mol). This is not due to any increase in polarizability, since ethane actually has both higher average and perpendicular polarizabilities than ethylene ($\alpha_\perp = 4.0$ Å^3 vs 3.6 Å^3), and in fact, theory finds roughly the same electrostatic attraction for C_2H_6 and C_2H_4. The conclusion is that a covalent interaction is responsible for the increased bond strength. The obvious difference between ethane and ethylene is the possibility of a significant π interaction, and Stöckigt et al.[11] find that 80% of the covalent interaction (about one-third of the total bond strength) does consist of donation from the C−C π orbital into the empty Al^+ 3pσ orbital. Donation into the 3pπ orbitals contributes another 10%. No discernible back-donation from the Al^+ 3s into the CC π^* orbital was found. A similar increase in bond dissociation energy occurs between $Mg^+C_2H_6$ and $Mg^+C_2H_4$.[33] From both these calculations it is clear that π donation makes a substantial contribution to the bonding.

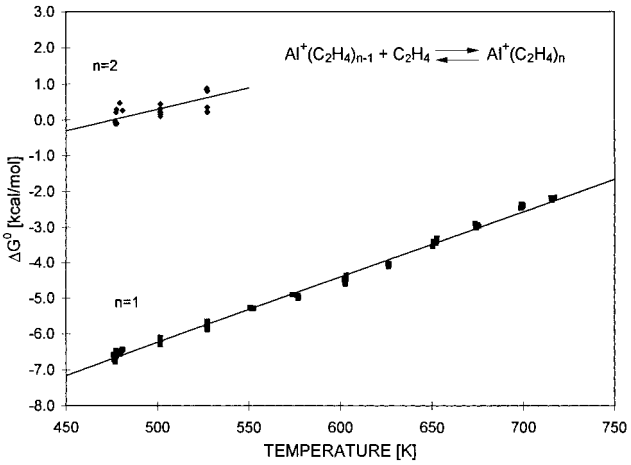

Figure 6. Plot of free energy vs temperature data for the $Al^+(C_2H_4)_{n-1} + C_2H_4 \rightarrow Al^+(C_2H_4)_n$ association reactions.

It is interesting to note that the second C_2H_4 ligand is bound about 40% less strongly than first (∼9 vs 15.5 kcal/mol; see Figure 6 and Table 4). No calculations have been done on this system, and it is unclear why such a reduction should occur. It is especially puzzling given that no such drop is observed in the second acetylene addition (discussed next).

$Al^+(C_2H_2)_n$. Figure 7 shows the equilibrium data for the addition of one and two C_2H_2 ligands to Al^+ along with the statistical mechanical fit to the data. Table 4 summarizes our experimental results (ΔH_T°, ΔS_T°, and bond dissociation energy). The theoretical bond dissociation energy of Stöckigt et al.[11] is also listed. The experimental and theoretical values (14.0 and 13.2 kcal/mol, respectively) agree quite well with theory calculating ∼95% of the binding. The ground-state structure from Stöckigt et al.[11] has the acetylene binding side-on to the Al^+, with Al−C distances of 2.75 Å (slightly shorter than the 2.85 Å length in the ethylene complex). The C_2H_2 molecule is nearly unperturbed, although the H−C−C bond angles do increase to 184° to move the H atoms away from the Al^+ ion.

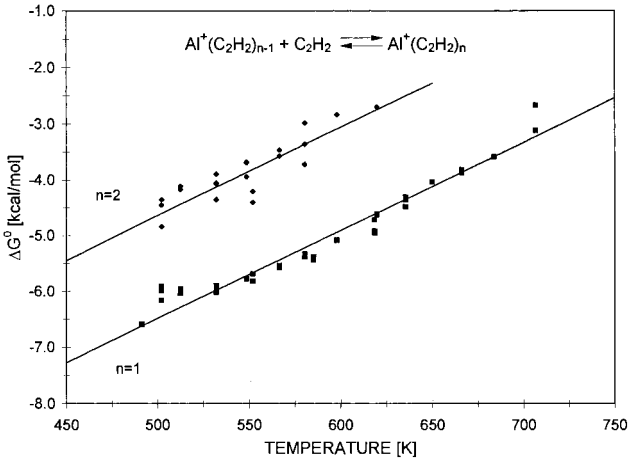

Figure 7. Plot of free energy vs temperature data for the $Al^+(C_2H_2)_{n-1} + C_2H_2 \rightarrow Al^+(C_2H_2)_n$ association reactions.

The metal−ligand interaction is very similar to that with C_2H_4. In both cases the bond has a large covalent component and in both cases it is primarily due to donation from the ligand π electrons into the empty 3pσ orbital on Al^+. The second π orbital on acetylene contributes only about 10% to the covalent attraction. As in C_2H_4, no back-donation from Al^+ to C_2H_2 is present. Interestingly, both theory and the present experiment find the $Al^+-C_2H_2$ bond strength to be similar to but slightly *weaker* than that with C_2H_4. The difference is small, ~1.1 kcal/mol (experimental) and 0.4 kcal/mol (theory), with a significant uncertainty in the absolute size, but the ordering seems robust. This ordering is unusual, as we are unaware of any other instance where ethylene binds more strongly to a metal ion. This point caused Stöckigt et al.[11] some concern, especially since their equilibrium experiments indicated that acetylene was slightly more strongly bound to Al^+. These were low-pressure, single-temperature experiments (a theoretical ΔS_T° correction was made), and the present results indicate the calculations are probably correct. The origin of such a small difference in binding is very difficult to determine and must be due to a combination of small differences in polarizability, donation from the C−C π orbital to the Al^+ σ orbital, and donation from the CH σ orbitals to the Al^+ p orbitals.

Calculations by Sodupe and Bauschlicher on the $Mg^+C_2H_2$ ion found a bond energy of 18.8 kcal/mol.[35] This is ~40% greater than the QCISD(T) calculations on $Al^+C_2H_2$, which is consistent with the relative Mg^+/Al^+ binding energies for the ligands discussed previously. The $Mg^+C_2H_4$ bond energy calculated at the same time was 18.6 kcal/mol, very similar to but slightly less than the acetylene value.

Conclusions

(1) Zero Kelvin bond association enthalpies and entropies for Al^+ ions (^1S, $3s^2$) coordinating with H_2, CH_4, C_2H_6, C_2H_4, and C_2H_2 have been measured using a high-pressure equilibrium technique. Data for four H_2, six CH_4, one C_2H_6, two C_2H_4, and two C_2H_2 ligands were obtained. First ligand bond strengths for the above ligands were 1.35, 6.05, 9.3, 15.0, and 14.0 kcal/mol, respectively.

(2) The bond strengths are uniformly much weaker than those between transition metal ions and the same ligands. This is attributed to repulsion due to the large filled Al^+ 3s orbital and a lack of low-energy, empty orbitals to accept electron density from the ligands. Calculations by Stöckigt et al. confirm this and show that most of the bonding is electrostatic except in C_2H_4 and C_2H_2, where the attraction is about half-covalent.

(3) Extensive calculations were done on the $Al^+(H_2)_n$ and $HAlH^+(H_2)_{n-1}$ ions. The bonding is similar to but much weaker than that found in the isovalent B^+ systems. Theory found the uninserted Al^+ clusters were weakly bound electrostatic species with calculated bond energies in good agreement with the present experiments. The inserted $HAlH^+$ ion is unstable with respect to the separated reactants, but calculations indicate that it is a minimum on the potential energy surface. The $HAlH^+$ ion forms partly covalent bonds with up to two additional H_2 ligands.

(4) Bonding to the Al^+ and Mg^+ core ions is similar for the ligands examined here. The Al^+·L BDEs were about 70% of the corresponding Mg^+·L values.

Acknowledgment. We gratefully acknowledge the support of the National Science Foundation under Grants CHE-9729146 and CHE-9551008; the partial support of the Air Force Office of Scientific Research under Grants F49620-96-1-0033 and F49620-96-1-0247; the Robert Welch Foundation; and the Petroleum Research fund (administered by the American Chemical Society) under Grant PRF No. 28190-AC6.

References and Notes

(1) Dalleska, N. F.; Tjelta, B. L.; Armentrout, P. B. *J. Phys. Chem.* **1994**, *98*, 4191.
(2) Stöckigt, D.; Hrušák, J.; Schwarz, H. *Int. J. Mass Spectrom. Ion Processes* **1995**, *149/150*, 1.
(3) Stöckigt, D.; Holthausen, M. C.; Koch, W.; Schwarz, H. *J. Phys. Chem.* **1995**, *99*, 5950.
(4) Uppal, J. S.; Staley, R. H. *J. Am. Chem. Soc.* **1982**, *104*, 1235.
(5) Hodges, F.; Armentrout, P. B.; Beauchamp, J. L. *Int. J. Mass Spectrom. Ion Phys.* **1979**, *29*, 375.
(6) Jarrold, M. F.; Bower, J. E. *J. Am. Chem. Soc.* **1988**, *110*, 70.
(7) Sodupe, M.; Bauschlicher, C. W. *Chem. Phys. Lett.* **1991**, *181*, 321.
(8) Bauschlicher, C. W.; Bouchard, F.; Hepburn, J. W.; McMahon, T. B.; Surjasamita, P.; Roth, L.; Gord, J. R.; Freiser, B. S. *Int. J. Mass Spectrom. Ion Processes* **1991**, *109*, 15.
(9) Stöckigt, D. *J. Phys. Chem. A* **1997**, *101*, 3800.
(10) Stöckigt, D.; Hrušák, J. *J. Phys. Chem.* **1994**, *98*, 3675.
(11) Stöckigt, D.; Schwarz, J.; Schwarz, H. *J. Phys. Chem.* **1996**, *100*, 8786.
(12) DePuy, C. H.; Gareyev, R.; Hankin, J.; Davico, G. E. *J. Am. Chem. Soc.* **1997**, *119*, 427.
(13) Kemper, P. R.; Bushnell, J. E.; Weis, P.; Bowers, M. T. *J. Am. Chem. Soc.*, in press.
(14) Sharp, S. B.; Gellene, G. I. *J. Am. Chem. Soc.*, in press.
(15) Kemper, P. R.; Weis, P.; Bowers, M. T. *Int. J. Mass Spectrom. Ion Processes* **1997**, *10*, 17.
(16) Bushnell, J.; Kemper, P. R.; Maitre, P.; Bowers, M. T. *J. Am. Chem. Soc.* **1994**, *116*, 9710.
(17) Kemper, P. R.; Weis, P.; Bowers, M. T. *J. Am. Chem. Soc.*, submitted.
(18) Bushnell, J.; Kemper, P. R.; Bowers, M. T. *J. Phys. Chem.* **1993**, *97*, 11628.
(19) Kemper, P. R.; Bowers, M. T. *J. Phys. Chem.* **1991**, *95*, 5134.
(20) Woon, D. E.; Dunning, T. H., Jr. *J. Chem. Phys.* **1993**, *98*, 1358.
(21) Frisch, M. J.; Trucks, G. W.; Schlegel, H. B.; Gill, P. M. W.; Johnson, B. G.; Robb, M. A.; Cheeseman, J. R.; Keith, T.; Petersson, G. A.; Montgomery, J. A.; Raghavachari, K.; Al-Laham, M. A.; Zakrzewski, V. G.; Ortiz, J. V.; Foresman, J. B.; Cioslowski, J.; Stefanov, B. B.; Nanayakkara, A.; Challacombe, M.; Peng, C. Y.; Ayala, P. Y.; Chen, W.; Wong, M. W.; Andres, J. L.; Replogle, E. S.; Gomperts, R.; Martin, R. L.; Fox, D. J.; Binkley, J. S.; Defrees, D. J.; Baker, J.; Stewart, J. P.; Head-Gordon, M.; Gonzalez, C.; Pople, J. A. *Gaussian 94*, revision C_2; Gaussian, Inc.: Pittsburgh, PA, 1995.
(22) (a) Bauschlicher, C. W.; Partridge, H.; Langhoff, S. R. *J. Chem. Phys.* **1989**, *91*, 4733. (b) Partridge, H.; Bauschlicher, C. W.; Langhoff, S. R. *J. Phys. Chem.* **1992**, *96*, 5350. (c) Bauschlicher, C. W.; Partridge, H.; Langhoff, S. R. *Chem. Phys. Lett.* **1990**, *165*, 272.
(23) Weis, P.; Kemper, P. R.; Bowers, M. T. *J. Phys. Chem. A* **1997**, *10*, 17.
(24) Bauschlicher, C. B.; Partridge, H. *Chem. Phys. Lett.* **1991**, *181*, 129.
(25) Bauschlicher, C. B.; Partridge, H.; Langhoff, S. R. *J. Phys. Chem.* **1992**, *96*, 2475.

(26) Bauschlicher, C. B. *Chem. Phys. Lett.* **1993**, *201*, 11.
(27) Moore, C. E. *Atomic Energy Levels*; Nat. Bur. Standards (U.S) circular 467, 1949.
(28) Gellene, G. I. Work in progress.
(29) Stöckigt, D. Private communication of $Al^+(CH_4, C_2H_6, C_2H_4, C_2H_2)$ vibrational frequencies.
(30) (a) Kemper, P. R.; Bushnell, J.; van Koppen, P.; Bowers, M. T. *J. Phys. Chem.* **1993**, *97*, 1810. (b) Armentrout, P. B.; Kickel, B. L. In *Organometallic Ion Chemistry*; Freiser, B. S., Ed.; Kluwer Academic Pub.: Dordrecht, The Netherlands, 1996.
(31) Schultz, R. H.; Armentrout, P. B. *J. Phys. Chem.* **1993**, *97*, 596.
(32) van Koppen, P. A.; Bushnell, J.; Kemper, P. R.; Bowers, M. T. *J. Am. Chem. Soc.* **1995**, *117*, 2098.
(33) Partridge, H.; Bauschlicher, C. B. *J. Phys. Chem.* **1992**, *96*, 8827.
(34) Bauschlicher, C. W.; Sodupe, M. *Chem. Phys. Lett.* **1993**, *214*, 489.
(35) Sodupe, M.; Bauschlicher, C. W. Chem. Phys. **1994**, *185*, 163.